IET Generation, Transmission & Distribution

WILEY

The Institution of Engineering and Technology

ORIGINAL RESEARCH OPEN ACCESS

Optimal Coordination of Active Distribution System Operation Supported With BESS Under Varying PV-Wind Generation and Load Demands

Asad Ali[1] | Hazlie Mokhlis[1,2] | Nurulafiqah Nadzirah Mansor[1] | Hasmaini Mohamad[3] | Nur Zawani Saharuddin[4] | Hussain Shareef[5,6]

[1]UM Power and Energy System Research Group (UMPES), Department of Electrical Engineering, Faculty of Engineering, Universiti Malaya, Kuala Lumpur, Malaysia | [2]Photonic Research Centre, Universiti Malaya, Kuala Lumpur, Malaysia | [3]Power System Planning and Operation Research Group (PoSPO), Faculty of Electrical Engineering, Universiti Teknologi MARA (UiTM), Shah Alam, Selangor, Malaysia | [4]Faculty of Electrical Technology and Engineering, Universiti Teknikal Malaysia Melaka (UTeM), Durian Tunggal, Melaka, Malaysia | [5]Department of Electrical and Communication Engineering, College of Engineering, United Arab Emirates University, Al Ain, United Arab Emirates | [6]Emirates Center for Mobility Research, United Arab Emirates University, Al Ain, United Arab Emirates

Correspondence: Hazlie Mokhlis (hazli@um.edu.my) | Nurulafiqah Nadzirah Mansor (afiqah.mansor@um.edu.my)

Received: 23 February 2026 | **Revised:** 15 June 2026 | **Accepted:** 5 July 2026

ABSTRACT

The growing penetration of photovoltaic and wind generation is reshaping traditional distribution networks into active distribution systems. Maintaining secure and efficient operation under variable generation and load conditions has become increasingly challenging. This study presents an optimal coordination framework for active distribution system operation that integrates battery energy storage systems with practical network control mechanisms, including on-load tap changers, switchable capacitor banks and feeder reconfiguration. To effectively manage the mixed nature of decision variables, a hybrid optimization strategy is developed in which the discrete firefly algorithm is employed to handle discrete control actions such as OLTC tap positions and network reconfiguration, while the generalized normal distribution optimization method is applied to continuous variables related to renewable energy sources, BESS power scheduling and capacitor bank sizing. This coordinated optimization allows renewable generation and energy storage to operate synergistically, mitigating intermittency effects without causing voltage violations or thermal overloading. Practical applicability is ensured by incorporating realistic operational constraints, including voltage and line current limits, radial network structure, OLTC operating ranges, BESS state-of-charge limits and safe switching requirements. The framework is assessed over a 24-h operating horizon to capture the dynamic interaction between load demand and renewable generation. Validation on the IEEE 69-bus system and the real Iran 59-bus distribution network demonstrates notable improvements in voltage regulation, loss reduction and operational cost, while preserving system reliability. The proposed coordination approach offers a feasible and implementable solution for managing renewable-rich active distribution systems.

1 | Introduction

The increasing penetration of renewable energy sources (RES), particularly photovoltaic (PV) and wind generation, is transforming conventional distribution networks into active distribution networks (ADNs) with bidirectional power flow and enhanced operational flexibility [1]. This transition is driven by rising electricity demand, environmental concerns, declining renewable energy costs, and global carbon reduction targets [2]. While RES integration offers significant economic and environmental benefits, their intermittent and stochastic nature introduces new operational challenges, including voltage fluctuations, feeder overloading, reverse power flow, and increased network losses [3, 4]. To address these challenges, ADNs are increasingly equipped with flexible control resources such as on-load tap changers (OLTCs), switchable capacitor banks (SCBs), network reconfiguration through tie-switch operation and battery energy storage systems (BESSs). OLTCs and SCBs provide voltage and reactive power regulation, while network reconfiguration reshapes power flow paths to reduce losses and improve load balancing [5–7]. BESS further enhances ADN flexibility by absorbing excess renewable generation and supplying power during peak demand, thereby mitigating RES variability [8]. However, the effective utilization of these resources requires coordinated operation; isolated control of individual devices may lead to conflicting actions and degraded system performance.

Numerous studies have investigated ADN operation using heuristic, metaheuristic, artificial intelligence and mathematical optimization approaches. Distribution network reconfiguration has been widely explored as an effective means of loss minimization and voltage improvement, [9, 10] while capacitor placement and reactive power management have also been studied extensively [11, 12]. Several works have considered RES allocation and BESS integration to improve system reliability and reduce operating costs [13, 14]. Stochastic and scenario-based methods have been applied to capture renewable uncertainty and load variability [15, 16]. Despite these efforts, many studies focus on optimizing a single control strategy or adopting simplified network models that do not fully capture AC power flow characteristics, limiting their practical relevance. More recent research has attempted to integrate multiple control actions within unified optimization frameworks. Coordinated optimization of network reconfiguration, OLTC operation, and distributed energy resource dispatch has been reported in [17–19], while multi-period and multi-objective formulations have been explored using mixed-integer nonlinear programming and evolutionary algorithms [20–22]. Although these approaches demonstrate improved system performance, practical operational constraints are often overlooked. Frequent feeder switching, unconstrained OLTC tap changes and unrestricted power export to the upstream grid are commonly assumed, despite their incompatibility with utility operating practices and equipment limitations [18, 23]. Furthermore, limited attention has been given to explicitly coordinating RES and BESS operation to restrict reverse power flow and enhance local energy utilization.

This paper proposes a coordinated and practically implementable optimization framework for ADN operation that simultaneously considers renewable generation, BESS, OLTC control, switchable capacitor banks and network reconfiguration. The framework ensures that RES and BESS operate synergistically to mitigate intermittency, maintain voltage stability, and limit power injection into the upstream grid.

The main contributions of this study are summarized as follows:

1. Development of an integrated coordination framework for active distribution system operation incorporating PV, wind generation, BESS, OLTCs, SCBs and feeder reconfiguration.
2. Formulation of a unified optimization model that jointly handles discrete operational decisions and continuous control variables under realistic technical constraints.
3. Explicit coordination of RES and BESS to suppress reverse power flow and improve local energy consumption.

The rest of the paper is structured in the following manner. In Section 2, the problem formulation and device modelling are presented. The hybrid optimization method is provided in Section 3. The test systems and simulation scenarios are described in Section 4. Section 5 presents the results and discussion. The conclusion of the paper is found in Section 6.

2 | Modelling Uncertainty and Problem Formulation

2.1 | Wind and Solar Energy

The Weibull distribution, X_υ presented in (1) is assumed to be able to accurately simulate the historical wind speed ω record in the following way [24].

$$X_\nu(\omega/h,\lambda) = \frac{h}{\lambda}\left(\frac{\omega}{\lambda}\right)^{h-1} e^{-\left(\frac{\omega}{\lambda}\right)^{h}} \tag{1}$$

The following formula can be used to determine the active power produced by the wind turbine (2) [25].

$$A_{wg} = \begin{cases} 0 & if\ \omega < \omega_{ci}\ or\ \omega > \omega_{co} \\ A_{wg}^{\max} & if\ \omega_{no} \le \omega \le \omega_{co} \\ A_{wg}^{\max}\frac{\omega-\omega_{ci}}{\omega_{no}-\omega_{ci}} & if\ \omega_{ci} \le \omega \le \omega_{no} \end{cases} \tag{2}$$

$$X(r) = \frac{r(a+b)}{r(a)\,r(b)} r^{a-1}(1-r)^{b-1} \tag{3}$$

The beta distribution in (3) models the solar radiation, r (W/m^2) as follows [26]. Additionally, the PV generator's generated active power can be computed as follows in (4):

$$A_{\mathrm{PV}} = \begin{cases} A_{\mathrm{PV}}^{\max}\left(\frac{r^2}{r_c \times r_{\mathrm{std}}}\right) & 0 \le r < r_c \\ A_{\mathrm{PV}}^{\max}\left(\frac{r}{r_{\mathrm{std}}}\right) & r_c \le r \le r_{\mathrm{std}} \\ A_{\mathrm{PV}}^{\max} & r_{\mathrm{std}} < r \end{cases} \tag{4}$$

where the values of r_c and r_{std} are set at 150 and 1000 W/m^2, respectively, to represent a specific radiation point and the solar radiation under standard conditions. For each test system, two PV-based DGs are modelled with a 24-h generation profile. In the 59-bus system, PV-based DGs with 3 MW capacity, a 0.95 power factor and 993 kVAR reactive power are placed on buses 22 and 39. Similarly, in the 69-bus system, PV DGs with the same specifications is located on buses 27 and 41. For wind-based DGs, one is modelled per system with a 24-h profile. In the 59-bus system, a 3 MW wind DG, operating at a 0.95 power factor and generating 993 kVAR, is located at bus 48 using the GWP47-750 kW turbine. In the 69-bus system, a similar wind DG is placed at bus 64, based on the PW56 turbine.

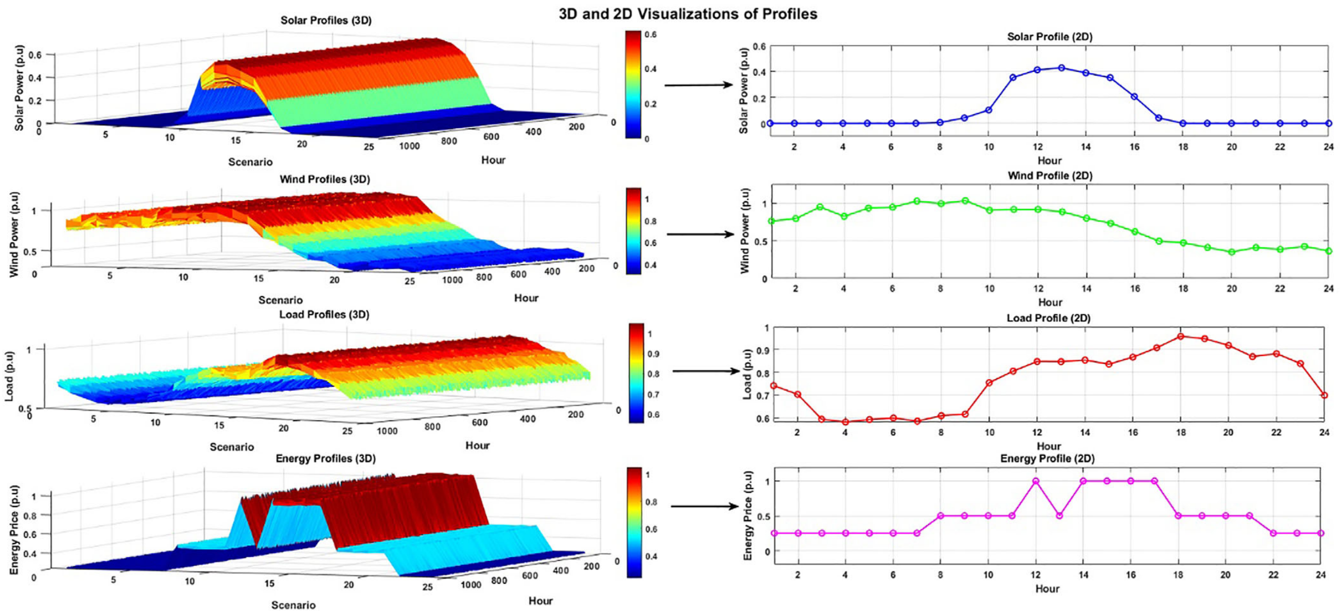

FIGURE 1 | Solar PV generation, wind power generation, load profile, and energy prices: BRM-selected scenario (left) vs QMCS-generated scenarios (right).

2.2 | Load Variation and Energy Prices

This research work models load power uncertainty, A_d(MW), using a normal distribution $X(A_d)$ with a defined mean value m_d(MW) and standard deviation s_d(MW), based on historical data in (5) as follows [27].

$$X\left(A_d\right) = \frac{1}{\sqrt{2\pi s_d}} e^{\left(-\frac{\left(A_d - m_d\right)^2}{2s_d^2}\right)} \tag{5}$$

Electricity price uncertainty, A_E ($/kWh), is represented using a normal distribution $X(A_E)$, characterized by a historical mean m_{U_E} and standard deviation s_{U_E} derived from historical records, represents in (6), as explained in [28].

$$X\left(A_E\right) = \frac{1}{\sqrt{2\pi s_{U_E}}} e^{\left(-\frac{\left(U_E - m_{U_E}\right)^2}{2s_{U_E}^2}\right)} \tag{6}$$

2.3 | Quasi Monte Carlo Simulation Methods

This study employs Quasi-Monte Carlo simulation (QMC) for scenario generation due to its faster convergence and greater efficiency compared to traditional Monte Carlo simulation (MCS) [29], especially in complex systems such as the 59-bus and IEEE 69-bus networks. QMC's utilizes low-discrepancy sequences, such as Sobol or Halton, to ensures uniform coverage of the input space, making it particularly suitable for capturing the variability of renewable energy systems (RES), including solar, wind and load profiles, and fluctuating energy prices. Unlike MCS, which relies on random sampling and converges at a slower $\frac{1}{\sqrt{N}}$ rate, QMC achieves faster convergence at approximately $\frac{1}{N}$ reducing computational time while maintaining accuracy. Furthermore, the integration of the point estimate method (PEM) complements QMC by minimizing computational effort through the use of the first few moments, making it well-suited for efficiently managing stochastic variables and improving precision in RES-based distribution network studies while accounting for dynamic energy pricing. Although QMCS generates a large number of scenarios (as shown on the right side of Figure 1) to accurately represent stochastic uncertainties, it significantly increases computational time for the optimization process. To address this challenge, the backward reduction algorithm (BRA) is applied to reduce the number of generated scenarios to a smaller, more manageable set while preserving their associated probabilities. Ultimately, the BRA method condenses the scenarios into a single representative scenario, as illustrated on the left side of Figure 1.

2.4 | Problem Formulation and Constraints

The proposed planning model is formulated as a two-stage MINLP multi-objective optimization problem that simultaneously minimizes active power loss, voltage deviation and operational costs. In the planning stage, the framework determines the optimal allocation and sizing of distributed resources such as PV, wind, BESS and SCBs. In the operation stage, the model suggests practically implementable strategies for network reconfiguration (NR) and OLTC settings, ensuring that line current and voltage limits are respected under real-world operating conditions. The overall structure of the proposed model is illustrated in Figure 2.

2.4.1 | Objective Functions

This study aims to minimize three objectives: active power loss, voltage deviation and operational cost of the system.

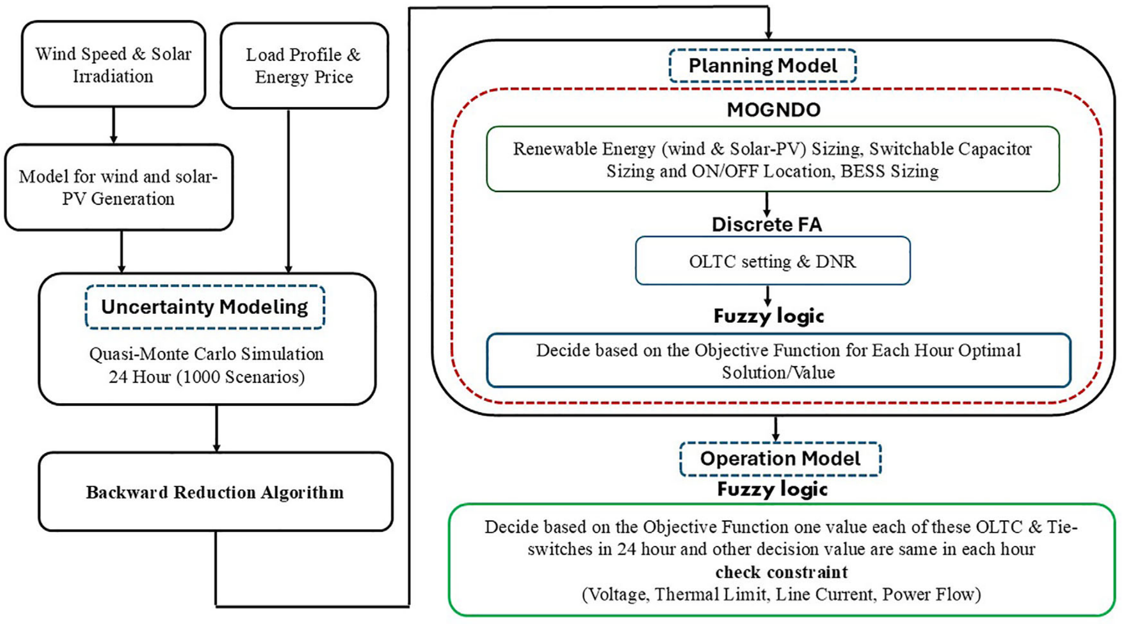

FIGURE 2 | Framework of the proposed model.

Object 1: Active Power Loss

The first objective focuses on reducing the total active power loss occurring in the distribution network. These losses are mainly caused by the resistance of the conductors through which current flows.

$$\text{Minimization } P_{\text{loss}} = \sum_{i=1}^{N_{\text{lines}}} R_i . I_i^2 \tag{7}$$

Here, R_i corresponds to the resistance of the line i, I_i is the associated line current, and N_{lines} refers to the number of lines in the system. Minimization of this loss directly contributes to improved efficiency and lower energy wastage.

Objective 2: Voltage Deviation

The second objective seeks to minimize bus voltage deviations relative to the nominal reference level, as pronounced variations can impair power quality and system component performance. The voltage deviation index is defined as:

$$\text{Minimization } V_{\text{dev}} = \sum_{j=0}^{N_{\text{buses}}} \left| V_j - V_{\text{ref}} \right| \tag{8}$$

Here, V_j refers to the voltage at the j^{th} bus, V_{ref} is the target reference voltage and N_{buses} denotes the total bus count. Reduced voltage deviation reflects better voltage regulation and more stable system operation.

Objective 3: Operational Cost

This objective is concerned with lowering total operating cost of the distribution network. It includes expenditures related to RES, BESS, SCB, OLTC adjustments, tie-switches operations, line losses and power imported from the main grid. The combined cost function is given by,

$$\text{Minimization } C_{\text{Total-Operat}} = C_{\text{Ren}} + C_{\text{Cap}} + C_{\text{BESS}} + C_{\text{OLTC}} + C_{\text{Tie-Switch}} + C_{\text{Power loss}} + C_{\text{Grid}} \tag{9}$$

The terms in this expression quantify the costs of the individual components, and minimizing the aggregate cost improves the overall economic efficiency of the distribution network.

2.4.2 | Constraints of Equality and Inequality

The formulation includes both equality and inequality constraints to ensure that control variables remain within acceptable operating limits. Equality constraints maintain specified relationships among variables, while inequality constraints define allowable bounds. Collectively, these conditions steer the optimization process toward stable and practically feasible solutions.

2.4.2.1 | Equality Constraints. Equality constraints are imposed to maintain power balance within the network, ensuring that the total active and reactive power generation equals the combined load demand and system losses.

$$\sum_{t\in T} \left(P_{\text{SS}}^T + \sum_{i\in N_{\text{ESS}}} P_{\text{dch}_i}^T + \sum_{i\in N_{\text{RES}}} P_{\text{RES}_i}^T - \sum_{i\in N_b} \left(P_{D_b}^T + P_{\text{loss}} \right) - \sum_{i\in N_{\text{ESS}}} P_{\text{ch}_i}^T \right) = 0 \tag{10}$$

$$\sum_{t\in T} \left(Q_{\text{SS}}^T + \sum_{i\in N_{\text{ESS}}} Q_{\text{dch}_i}^T + \sum_{i\in N_{\text{RES}}} Q_{\text{RES}_i}^T + \sum_{i\in N_b} Q_{\text{SCB}_i}^T - \sum_{i\in N_b} \left(Q_{D_b}^T + Q_{\text{loss}} \right) - \sum_{i\in N_{\text{ESS}}} Q_{\text{ch}_i}^T \right) = 0 \tag{11}$$

Here, P_{sub} and Q_{sub} represent the active and reactive power supplied by the main substation, while P_D and Q_D denote the active and reactive power demands. P_{loss} and Q_{loss} correspond to network losses. The terms $P_{t,\text{chi}}$, $P_{t,\text{disch}}$, $Q_{t,\text{chi}}$, and $Q_{t,\text{disch}}$, describe the charging and discharging power of the energy storage device, and Q_{SCB} represents the reactive power of the switchable capacitor bank.

2.4.2.2 | Inequality Constraints. Inequality constraints represent the operational limits of power system equipment and components, as well as security restrictions on transmission lines and load buses.

$$P_{\text{SS}}^{\min} \le P_{\text{SS}} \le P_{\text{SS}}^{\max}; \qquad Q_{\text{SS}}^{\min} \le Q_{\text{SS}} \le Q_{\text{SS}}^{\max} \tag{12}$$

$$P_{\text{RES}_i}^{\min} \le P_{\text{RES}_i} \le P_{\text{RES}_i}^{\max}; \qquad Q_{\text{RES}_i}^{\min} \le Q_{\text{RES}_i} \le Q_{\text{RES}_i}^{\max} \tag{13}$$

$$\sum_{i=1}^{N_{\text{RES}}} P_{\text{RES},i} \le 0.9 * P_D \tag{14}$$

$$\sum_{i=1}^{N_{\text{RES}}} Q_{\text{RES},i} \le 0.9 * Q_D \tag{15}$$

$$\sum_{i=1}^{N_{\text{SCB}}} Q_{\text{SCB},i} \le 0.9 * Q_D \tag{16}$$

$$V_i^{\min} \le |V_i| \le V_i^{\max} \tag{17}$$

$$S_l^t \le S_l^{\max} \tag{18}$$

$$n_l \le N_b - 1 \tag{19}$$

$$\det(A) = \begin{cases} 1 \text{ or } -1, & \text{(radial network)} \\ 0, & \text{(Not radial)} \end{cases} \tag{20}$$

$$\text{SoC}_j^t = \text{SoC}_j^{t-1} + \frac{\eta_j P_{\text{dch}_j}^t}{E_j^{\max}} - \frac{P_{\text{ch}_j}^t}{\eta_j E_j^{\max}} \tag{21}$$

$$SoC_{j(\text{ini})} = \text{SoC}_j^{t-1} = 2.0 \text{ MWh} \tag{22}$$

$$0.2 * E_j^{\max} \le \text{SoC}_j \le 0.9 * E_j^{\max} \tag{23}$$

$$0 \le P_{\text{ch}_j}^t \le 0.2 \text{ MW and } 0 \le P_{\text{dch}_j}^t \le 0.2 \text{ MW} \tag{24}$$

$$0 \le Q_{\text{ch}_j}^t \le 0.2 \text{ MVAR and } 0 \le Q_{\text{dch}_j}^t \le 0.2 \text{ MVAR} \tag{25}$$

$$\left|I_{ij}\right| \le z_{ij} I_{ij,\max}, \qquad \forall ij \in \Phi_{line} \tag{26}$$

Each line's absolute value of the current $|I_{ij}|$ is guaranteed by the inequality to not be more than the product of z_{ij} and, $I_{ij,\max}$. The set of all branches or lines in the network is denoted by Φ_{line}. Therefore, this restriction is applicable to all the system's lines *ij*.

3 | Methodology

This paper analyses the impact of non-dispatchable solar PV-DG and wind-DG, which inject active and reactive power to reduce power losses. Simulations are conducted on a real 59-bus practical network and the IEEE 69-bus test system over a 24-h period. To account for uncertainties in solar and wind generation, load profiles, and energy prices, the QMC method generates 1000 scenarios. However, handling such a large number of scenarios increases computational complexity, which is mitigated using the BRA shown in Figure 1.

This study proposes a multi-objective hybrid optimization (MOHO) framework for the planning and operation model, as illustrated in Figure 2. The framework integrates the DFA for identifying optimal tie-switch configurations and OLTC settings, with the GNDO for determining the optimal sizes of wind, solar PV, BESS and SCBs. The methodology is tested on the IEEE 69-bus system and the real Iran 59-bus system. A multi-objective Pareto optimization approach is applied to minimize active power loss, voltage deviation and operational cost, ensuring enhanced efficiency and reliability in smart grid operation. One major challenge in solving multi-objective optimization problems is handling the Pareto front (PF), which offers a range of optimal solutions, complicating the selection of a single solution for each hour. Numerous studies have explored methods to determine the best compromise solution. This paper employs the fuzzy set method to identify the optimal compromise solution from the PF generated by MOHO, using Equation (27) for membership functions [30].

For OPC, APL and VD (minimizing functions),

$$\mu_j = \begin{cases} 1, & F_j \le F_j^{\min} \\ \frac{F_j^{\max} - F_j}{F_j^{\max} - F_j^{\min}}, & F_j^{\min} < F_j < F_j^{\max} \\ 0, & F_j \ge F_j^{\max} \end{cases} \tag{27}$$

The membership function represents F_j, the *j*th objective function, with $F_j^{\min}$ as its minimum value. The normalized membership function is then calculated using Equation (28). *M* represents the number of solutions in the Pareto front (PF), and the solution with the highest μ^k value is selected as the best compromise solution.

$$\mu^k = \frac{\sum_{j=1}^{3} \mu_j^k}{\sum_{l=1}^{M} \sum_{j=1}^{3} \mu_j^l} \tag{28}$$

3.1 | Multi-Objective Hybrid Optimization

In this study, the hybrid optimization algorithm with a multi-objective is introduced to solve multi-objective issues more efficiently. Widely used algorithms, such as MOPSO or NSGA-II, can encounter issues such as convergence problems and traps of local optima, particularly in a large search space or when the number is more than five, and six variables, which lead to suboptimal solutions. The proposed method can be utilized to deal with these drawbacks. MOHO model. In this research, a hybrid model is proposed that integrates the generalized normal distribution optimization (GNDO) algorithm with the discrete firefly algorithm (DFA). Figure 3 shows how this can be developed. The discrete decision variables, such as NR and OLTC settings, are appropriate. GNDO is a good fit where continuous

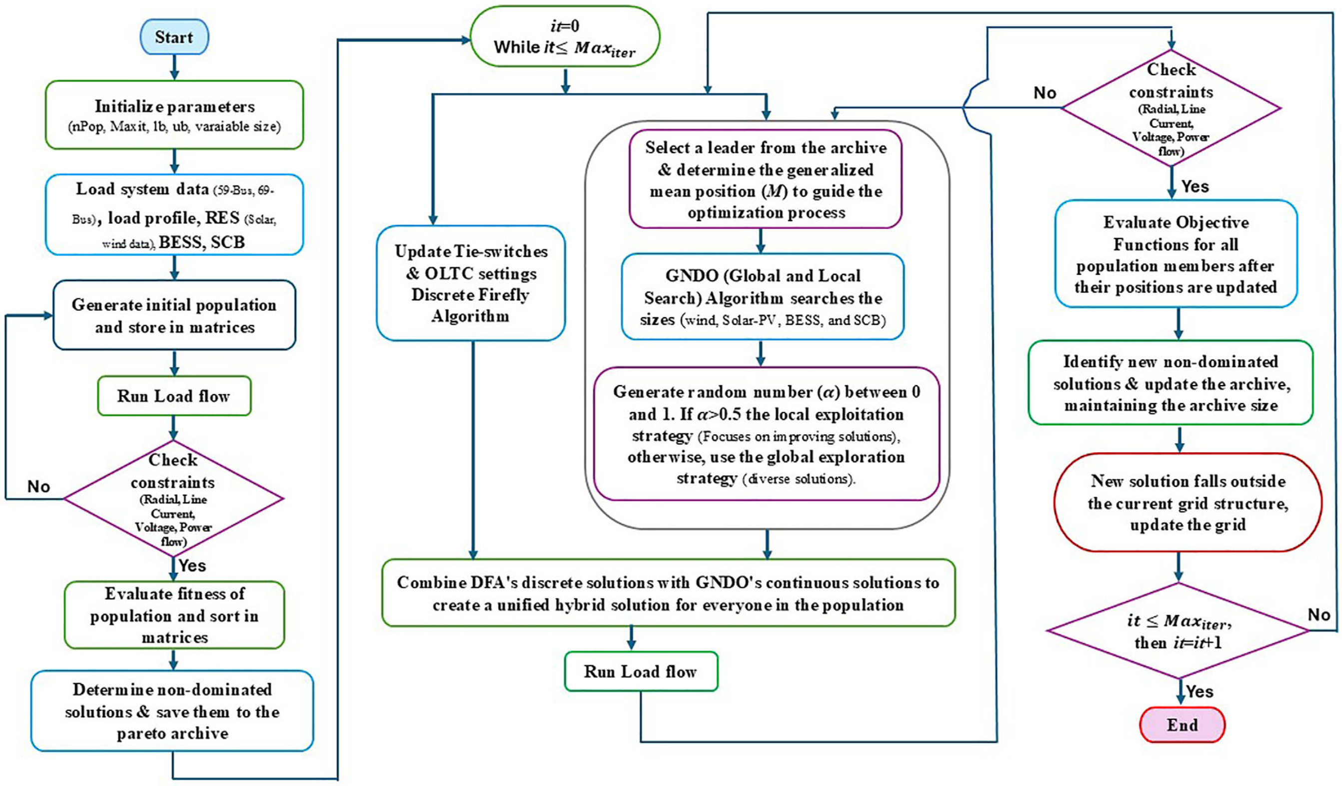

FIGURE 3 | Proposed MOHO framework for multi-objective distribution system optimization.

control variables need to be optimized, which include RES, BESS sizing and SCB sizing problems. The hybrid algorithm that one gets is called DFA-GNDO and beats conventional multi-objective optimization techniques like MOPSO, MOGWO and MOHHO by producing high-quality Pareto fronts of better quality and variety. Moreover, the performance of GNDO was proven in 35 benchmark case studies of mathematical problems and engineering problems, based on such performance measures as generational distance (GD), inverted generational distance (IGD), maximum spread (MS), etc. These outcomes show the strength and efficiency of the recommended method in the case of theory analysis and practice [28, 31]. Therefore, the hybrid optimization framework suggested is an effective solution to multi-objective optimization problems. This study is concerned with the planning and functioning of a multi-period system 24/7. First, the data of solar irradiation and wind speed are input into solar-PV and wind power generation models. These outputs, along with the load profile and energy price values, are used in a QMC simulation to generate 1000 scenarios. Due to computational limitations, a single representative scenario is selected using the backward reduction algorithm that is shown in Figure 1.

In the planning stage, a multi-objective optimization framework based on MOHO is employed. Within this framework, the GNDO algorithm is applied to determine the optimal sizing of continuous variables such as solar-PV, wind, BESS and switchable capacitors. For discrete decision variables, including tie-switch positions for network reconfiguration and OLTC tap settings, the DFA is used due to its effectiveness in handling discrete problems and its advantage of not requiring parameter tuning. Since the planning model is performed on a 24-h basis, the tie-switch positions and OLTC settings are further refined for practical operation. The OLTC regulates the grid-side voltage by adjusting the transformer tap settings, which are assumed to have 17 positions (from −8 to +8) [32], allowing voltage changes within the range of −5% to +5%. The voltage limits are set between a maximum of 1.05 p.u. and a minimum of 0.95 p.u., ensuring voltage stability by compensating for load and generation variations in the grid. Fuzzy logic is then applied to consolidate the hourly variations into a single optimal setting for the 24-h period, while the other decision variables (PV, wind, BESS and capacitors) are fixed in size. For each hour, the system supplies power according to load demand and solar/wind generation, with the BESS charging and discharging as needed to balance the supply-demand gap. The model evaluates the tie-switch positions and OLTC settings for each hour and identifies the best combinations according to the defined objective function.

In the operation stage, fuzzy logic is used to select one optimal tie-switch and OLTC combination from the 24 possible hourly results. This ensures that a single configuration is chosen as the most suitable throughout the day. The selected tie-switch configuration is then validated to determine which switches should remain closed or opened, while ensuring that practical constraints such as thermal line limits, line current capacities, voltage limits and radiality are satisfied.

4 | Results and Discussion

4.1 | Test System

This paper analyses the efficiency of the suggested planning and operation model in the optimization of the size of RES such as

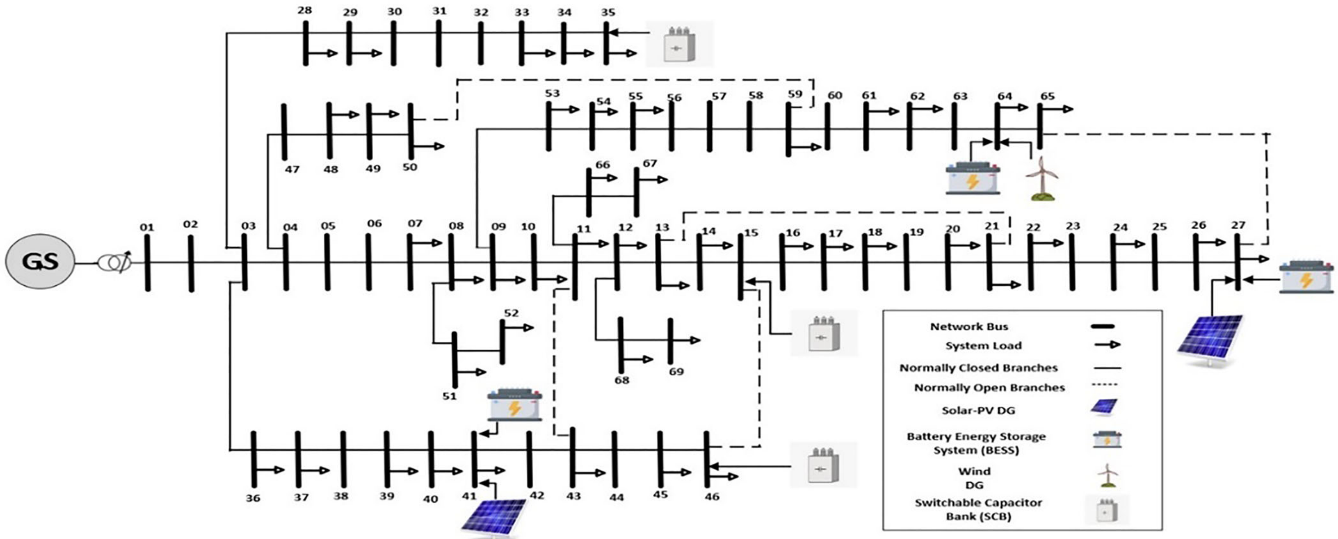

FIGURE 4 | Optimal source allocation in the 69-bus distribution system configuration.

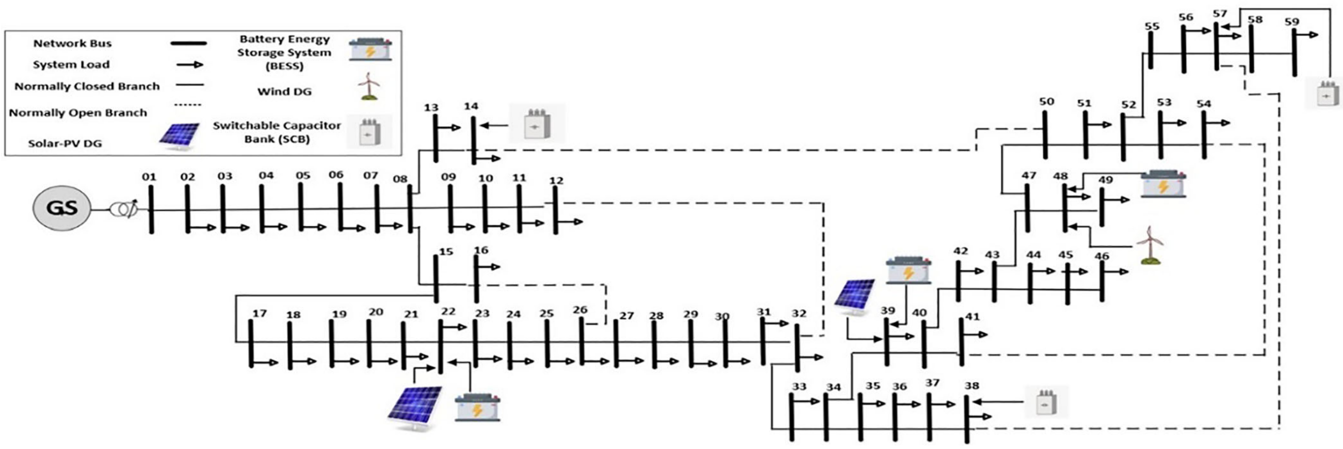

FIGURE 5 | Optimal source allocation in the Iran 59-bus distribution system configuration.

wind, solar PV, BESS and SCB and in the scheduling of RES and BESS with reduced OLTC changes. As contrasted to the planning models that are currently found in the literature, the operational model also uses a viable switching sequence and considers all the constraints at the same time, reducing three strategic goals: active power loss, voltage deviation and operational cost. The methodology is applied to two systems [33], the IEEE 69-bus system (shown in Figure 4) and the actual Iran 59-bus radial distribution system (RDS), shown in Figure 5.

The scenarios are as follows and are compared to MOPSO and MO-DFA-GNDO.

a. Base case
b. Integration of RES, BESS, SCB, OLTC and network reconfiguration (NR).

These situations reveal how the model can be used to increase sustainable energy integration without compromising operational limits.

4.2 | Simulation Results

This part will test the proposed MOHO procedure (MO-DFA-GNDO) against the existing multi-objective particle swarm optimization (MOPSO) approach and the base case scenario. The optimal decision variables taken into account in the analysis are the variables of RES, BESS, SCB sizing, OLTC settings and network reconfiguration, which are combined with the switching sequence process. The aim of this study is to single out one good configuration of one tie-switch position and OLTC setting, which will be implemented once a day, to make the operational strategy practically feasible. The suggested method is experimented on a 69-bus test system, and the actual distribution network of Iran 59-bus and the results are compared to those found with the use of MOPSO.

Figure 6 shows a total power analysis of the 59-bus and 69-bus systems in 24 h (MO-DFAGNDO), demonstrating how the power is distributed among various sources of energy both in the active and the reactive mode. The active power load demand, power losses and supply contributions of solar PV, wind, BESS and the

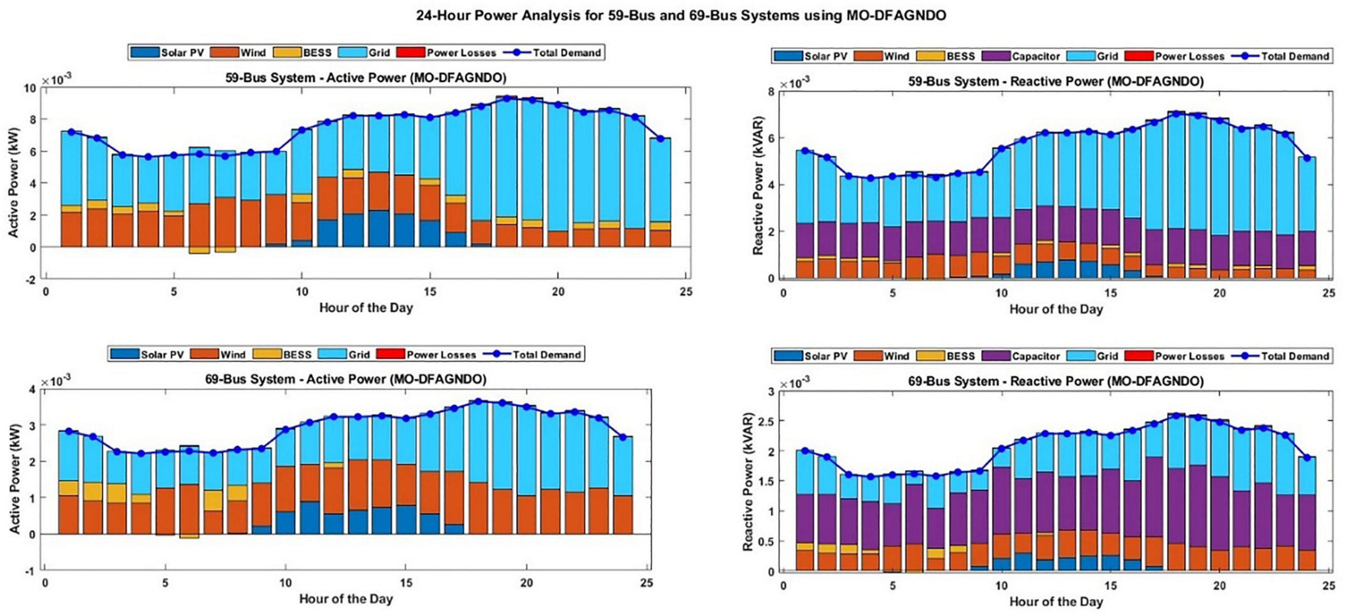

FIGURE 6 | Active and reactive power load demand and supply for the 59-bus and 69-bus systems using MO-DFAGNDO.

grid are shown on the left side of the figure, and the reactive power load demand and supply are shown on the right side of the figure. The upper row is 59-bus system, and the lower one is 69-bus system. The black line is the aggregate demand across the day and the red bars are the losses of power. These energy resources together supply the residual demand, which depicts the ability of the MO-DFAGNDO approach to not only minimize power losses but also to optimize the energy assets distribution. The results indicate that renewable generation and capacitor bank support of reactive power are used more efficiently and lead to an increase in system efficiency and stability.

Lastly, three main goals, which are active power losses, voltage deviations and cost reduction of operation, are analysed to determine the technical, economic, and environmental impacts on the performance of a system. Figure 7 shows the 3D Pareto fronts of MOPSO (left) and MO-DFA-GNDO (right) to 59-bus system (top) and 69-bus system (bottom). The blue markers refer to the non-dominated Pareto solutions of all three objectives, whereas the red marker refers to the best compromise solution calculated by the fuzzy decision-making. The MO-DFA-GNDO approach generates a smoother and more uniform Pareto front, which implies better convergence and diversity of the trade-off surface. These findings show that it is effective in reaching a balanced optimization between system reliability, technical performance and cost effectiveness, which is better.

Figure 8 shows the 24-h operation performance comparison of the base case, MOPSO, and the proposed hybrid MO-DFA-GNDO approach of the real 59-bus distribution system in Iran. The evaluation is based on three main objectives, such as active power loss, voltage deviation and operational cost. The hybrid approach beats the MOPSO, as well as the base scenario, in the way of providing more efficiency and voltage regulation in changing load situations throughout the day. To be more exact, the total active power loss declines to 92.1 kW with the help of the hybrid method compared to 118.4 kW in the base case and 104.6 kW with MOPSO, which is 22.2% lower than the base case and 10.6% improvement over MOPSO. Equally, the highest deviation in voltage is minimized to 0.0091 p.u. (base) and 0.0091 p.u. (MOPSO) with the hybrid approach, which is 15.7% lower than that of MOPSO. On the side of operation cost, the daily spending decreases to 1568 with the hybrid model, which is 8.6% less than that spent by MOPSO. These findings indicate that the proposed hybrid optimization structure is efficient in balancing technical performance and economic efficiency with lower losses, better voltage stability and cheaper operating costs and can be practically used in real-world distribution networks.

Figure 9 compares the total daily performance of the three scenarios, citing the percentage improvements that have been made by the proposed hybrid MO-DFA-GNDO algorithm. The loss of active power and voltage deviation and the cost of operation per day of each panel, both of which are shown as bar charts and trendlines of the differences with MOPSO. The hybrid strategy is always the lowest in all measures, showing that it is better optimized. Specifically, there is a 10.6 percent decrease in total daily active power loss, voltage deviation is better (15.7 percent), and the operating cost is lower (8.6 percent) than MOPSO. These findings highlight the fact that the hybrid algorithm can offer quicker convergence and a higher quality Pareto solution, leading to greater operational efficiency and better voltage regulation. The combination of the DFA and GNDO provides an opportunity to optimally explore and exploit the space of solutions to provide a strategy that is not only technically sound, but also economically feasible to use in the active operation of a distribution system.

Figure 10 shows the hourly change of active power loss, voltage deviation and operation cost of the base case, MOPSO and the suggested hybrid MO-DFA-GNDO algorithm on the IEEE 69-bus distribution system. Throughout the 24-h operating cycle, the hybrid approach has continuously lower values in the objective function than MOPSO and the base configuration. The active power loss reduces significantly from an average of 130 kW in the

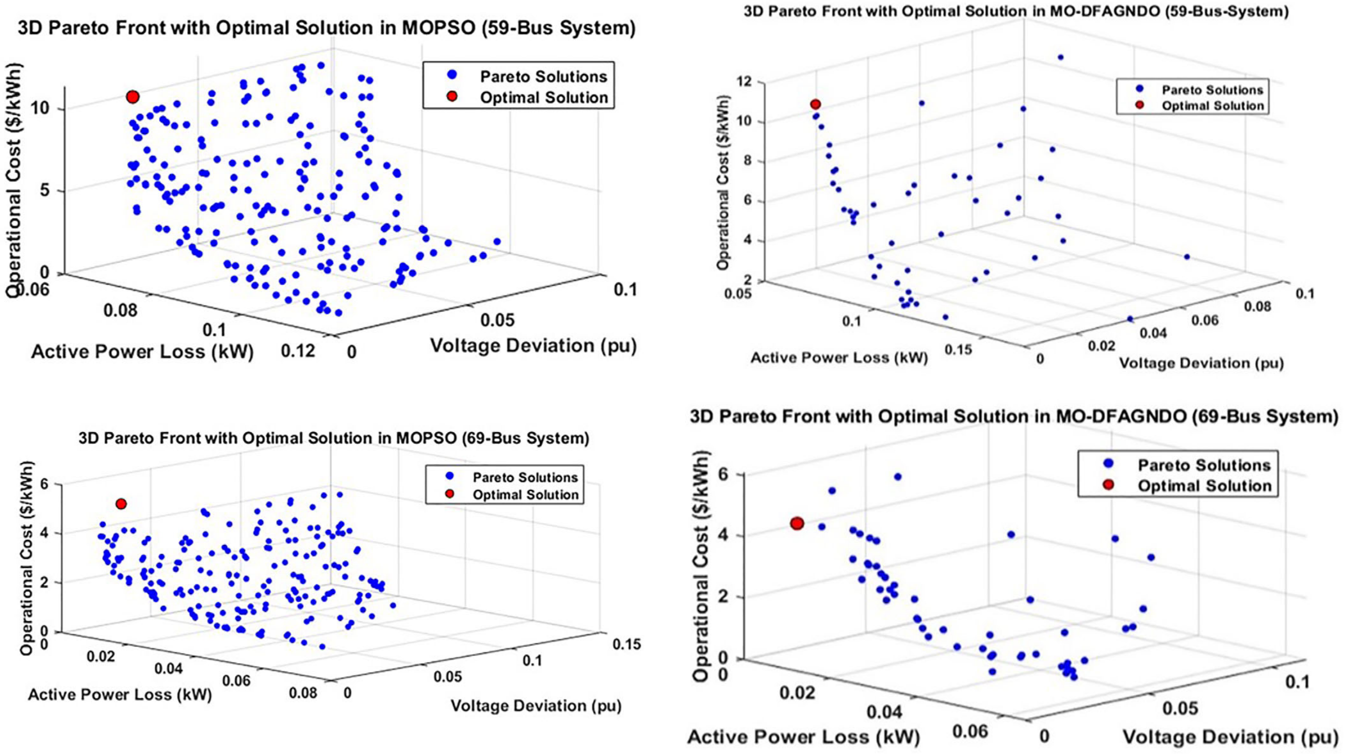

FIGURE 7 | Pareto fronts for MOPSO and MO-DFAGNDO on 59-bus and 69-bus networks.

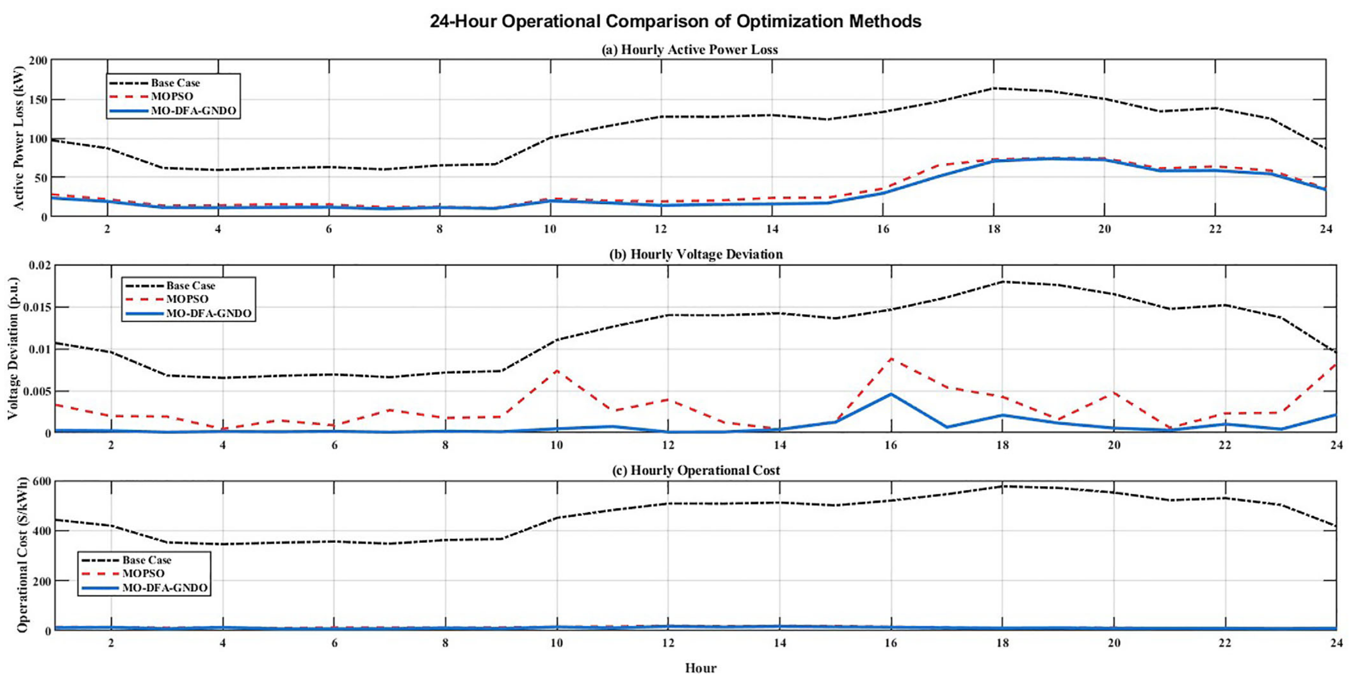

FIGURE 8 | Comparison of hourly performance for all three objective functions using the base case, MOPSO and hybrid (MO-DFA-GNDO) in the 59-bus.

base case to 18.6 kW in the case of MOPSO and further to 14.7 kW in the case of MO-DFA-GNDO, with an overall improvement of about 88.7 and 21 percent over the base case and MOPSO, respectively. In a similar fashion, the voltage deviation decreases in the base case from 0.045 to 0.0062 p.u. with MOPSO and the hybrid method, respectively, which is reduced by approximately 89 and 22 percent., respectively. On operational cost, the suggested algorithm reduces the total cost of 185$/kWh (base) to

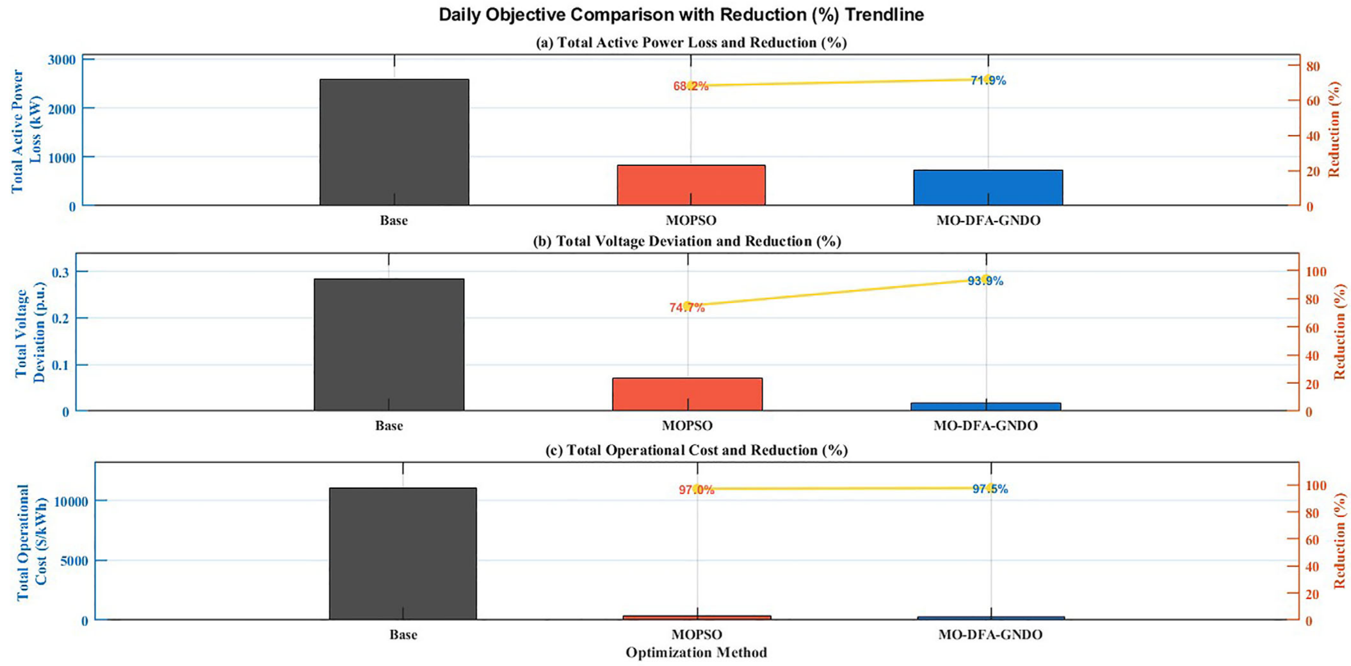

FIGURE 9 | Comparison of daily performance metrics and reduction trends for all three objective functions under the hybrid (MO-DFA-GNDO) method in the 59-bus distribution network.

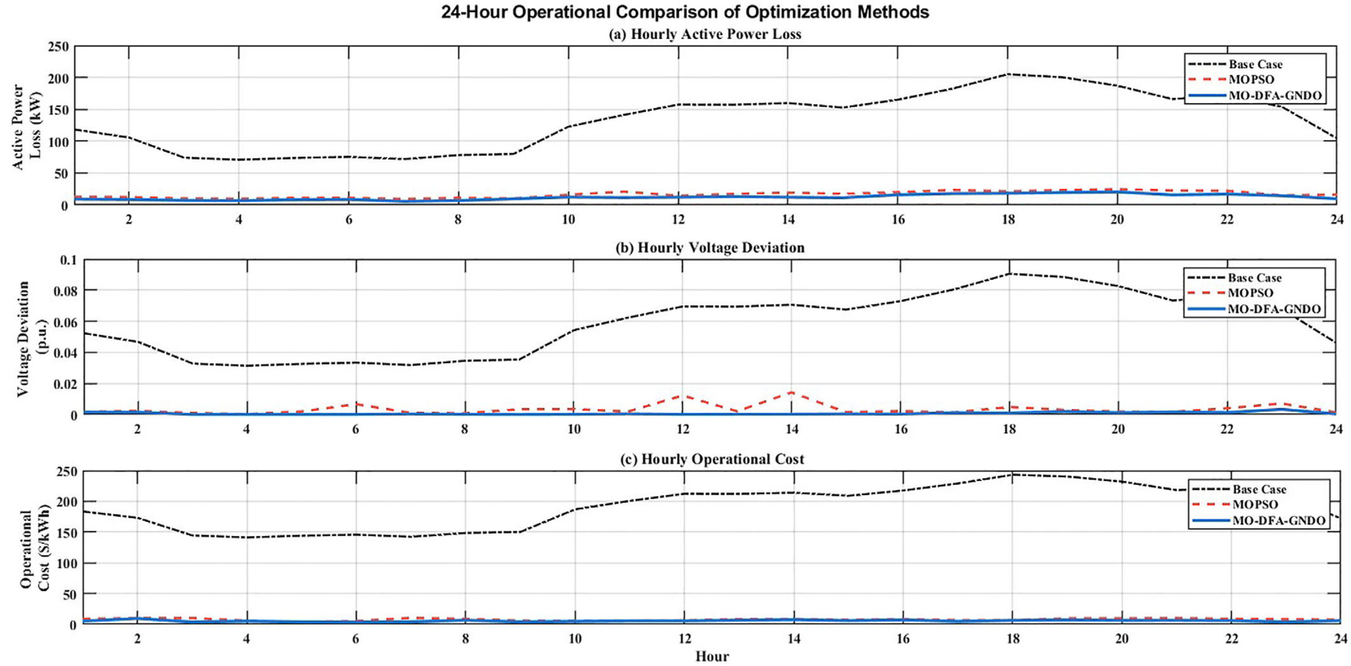

FIGURE 10 | 24-h performance of base case, MOPSO and hybrid (MO-DFA-GNDO) for all three objective functions in the 69-bus.

20$/kWh (MOPSO) and 15$/kWh (MO-DFA-GNDO), which is a reduction, respectively, of 91.9 and 25 percent of the base and MOPSO. Convergence is consistently quicker, voltage stability is enhanced, and it is more economical and still more reliable over the 24 h of the hybrid method compared to the non-hybrid approach.

Figure 11 shows the daily comparison of total active power loss, voltage deviation and operational cost in aggregate and trendlines depicting the percentage reduction of each method of optimization. The findings clearly show that the hybrid MO-DFA-GNDO approach has a higher level of performance than the MOPSO and the base scenario. In particular, the total power loss

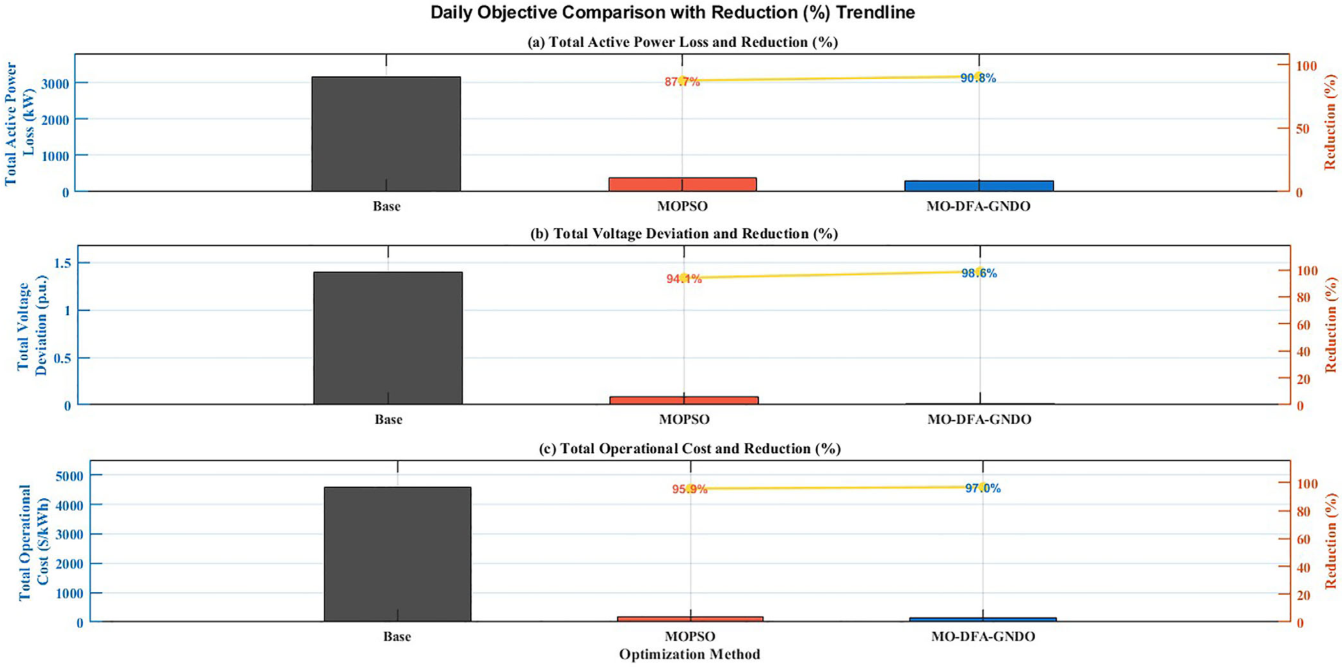

FIGURE 11 | Comparison of daily performance metrics and reduction trends for all three objective functions under the hybrid (MO-DFA-GNDO) strategy in the 69-bus distribution system.

per day of active operation is reduced in the base case of about 3100 to 380 kW with MOPSO and even more to 285 kW with the help of MO-DFA-GNDO, which is a reduction of 87.7 and 90.8 percent, respectively. On the same note, total voltage deviation decreases by 1.45 to 0.085 p.u. (MOPSO) and 0.058 p.u. (MO-DFA-GNDO) corresponding to decreases of 94.1% and 98.6%. Regarding the cost of operation, the hybrid option reduces the operation expenses by 95.9 and 97.0 percent, that is, the difference between the operation cost of $4800 (base) and the operation cost of $195 (MOPSO) and the operation cost of $145 (MO-DFA-GNDO). It is these drastic advancements that affirm that the hybrid algorithm not only improves the efficiency of the networks and minimizes technical losses, but also more effectively optimizes the overall day-to-day performance of the operations as compared to the traditional MOPSO approach.

A comprehensive comparison between the base case, MOPSO, and the suggested hybrid MO-DFA-GNDO approach under peak load conditions (18:00) to the IEEE 69-bus system and the real Iran 59-bus network is given in Table 1. The analysis includes technical, electrical, and economic parameters, such as active power loss, voltage deviation, operational cost, line currents and bus voltage magnitudes, which are evaluated in comparison with operational limits (maximum voltage of 1.05 p.u. and minimum of 0.95 p.u.).

In the case of the IEEE 69-bus system, the hybrid solution is much better, with an active power loss of 18.24 kW in the hybrid solution (out of 204.97 kW in the base case), a reduction of 91.1% with the hybrid solution plus an incremental improvement of 14.4 compared to MOPSO. The decrease in voltage deviation is 0.0905 to 0.0097 p.u. indicating a reduction of 98.9 percent compared to the base case and 80.2 percent compared to MOPSO. There is also a significant reduction in the operational cost of $243.18/h to an amount of 6.40/h of 97.4 percent. The maximum voltage stays approximately 1.003 p.u., which is approximately 4.47% less than the maximum value, whereas the minimum voltage is increased to 0.9891 p.u., which is approximately 4.12% larger than the minimum value. Also, in the Iran 59-bus system, the hybrid algorithm reduces the active power loss, voltage deviation and operational cost at 55.8%, 88.1% and 98.2% of the base case, respectively, and has additional gains of 3.0%–10.8% over MOPSO. Line currents do not exceed their rated values (400 and 350 A) and therefore there is thermal security. The maximum voltages are reduced by a small margin (approximately 4.5 percent of the limit) and minimum voltages go up by approximately 4.4 percent, which is a positive indication that the voltages are maintained in all buses. Additionally, it is evident that the results indicate that the presented hybrid MO-DFA-GNDO approach promotes better performance of the system by increasing and, at the same time, decreasing technical losses and cost-effective functioning, not to mention meeting the voltage and current restrictions. This justifies its relevance to real-life distribution networks and standard benchmark systems.

Table 2 provides a detailed result of hourly and daily optimization strategies based on the hybrid MO-DFA-GNDO method to 59 bus Iran versus IEEE 69-bus networks illustrating how the effective balance between practicality of the system operation and its performance is achieved. The hourly reconfiguration in the Iran 59-bus system reduces 2586 kW (base case) of active power loss to 727.1 kW, and the daily optimization, at 779.4 kW, retains almost 97 of the loss reduction achieved by hourly switching. The difference in voltages becomes significantly better, from 0.283476 to 0.01743 p.u. (hourly) and 0.01542 p.u. (daily) and the overall cost of the daily operation reduces by 97 percent. Equally, in the case of the IEEE 69- bus system, the active power loss is lowered to 290.6 kW instead of 3173 kW (hourly) and

TABLE 1 | Performance comparison at peak hour (18:00) for IEEE 69-bus and Iran 59-bus systems.

System	Objective	Base case	MOPSO	MO-DFA-GNDO	Reduction (%) vs. base	Reduction (%) vs. MOPSO
IEEE 69-bus	Active power loss (kW)	204.97	21.30	18.24	91.1%	14.4%
	Voltage deviation (p.u.)	0.0905	0.00489	0.00097	98.9%	80.2%
	Operational cost ($/kWh)	243.18	6.74	6.40	97.4%	5.1%
	Max. line current (A)	400	128.6	120.6	59.8%	6.2%
	Max. voltage (p.u.)	1.05	1.004	1.003	4.47%	0.10%
	Min. voltage (p.u.)	0.95	0.9869	0.9891	4.12%	0.09%
Iran 59-bus	Active power loss (kW)	160.17	72.97	70.79	55.8%	3.0%
	Voltage deviation (p.u.)	0.01756	0.00427	0.00209	88.1%	51.1%
	Operational cost ($/kWh)	570.30	11.45	10.20	98.2%	10.8%
	Max. line current (A)	350	172.4	165.3	52.8%	4.1%
	Max. voltage (p.u.)	1.05	1.0029	1.0028	4.51%	0.10%
	Min. voltage (p.u.)	0.95	0.9919	0.9923	4.45%	0.04%

TABLE 2 | Comparison of hourly vs daily reconfiguration performance of MO-DFA-GNDO.

Metric	Base case	Hourly optimization	Daily optimization (proposed)	Performance deviation (%) from base-hourly/base-daily
Active power loss (kW) in Iran 59-bus	2586	727.1	779.4	71.9/69.9
Voltage deviation (p.u.) in Iran 59-bus	0.283476	0.01743	0.01541733	93.9/94.6
Operational cost ($/day) in Iran 59-bus	11,042	273.592	308.022	97.5/97.2
Active power loss (kW) in IEEE 69-bus	3173	290.64	547.6	90.8/82.7
Voltage deviation (p.u.) in IEEE 69-bus	1.402789	0.01897	0.1445	98.6/89.7
Operational cost ($/day) in IEEE 69-bus	4591.66	136.335	161.88	97.0/96.5
Number of switch changes	N/A	24	1	−95.8%
OLTC tap changes	N/A	24	1	−95.8%
Maintenance cost	N/A	1.0	0.05	−95%

547.6 kW (daily), voltage deviation is minimized to 0.01897 p.u. instead of 1.4028 and 0.1445 p.u., and costs of operation are reduced to $136.3 and $161.9 per day as compared. Even though the hourly scheme has a little bit lower losses and deviations, it necessitates 24 tie-switch and OLTC tap operations per day, which in actual distribution grids is operationally impractical due to higher wear and tear, higher maintenance expenses, and heightened reliability risks. By comparison, the proposed daily operation is almost as effective with just a single switching and OLTC adjustment each day, which significantly decreases the switching load and maintenance needs by more than 95% and maintains more than 90 percent of the technical advantages. This shows that there is a practically viable, computationally efficient and economically sustainable solution of MO-DFA-GNDO framework, which considers the benefits of dynamic reconfiguration, and yet remains not impractical at the expenses of having to change every hour but is viable to support the current smart distribution system.

Figure 12 shows the hourly and daily best tie-switch and OLTC settings that were obtained using the proposed hybrid MO-DFA-GNDO algorithm on the IEEE 69-bus system, along with the actual 59-bus Iranian distribution network system. It is demonstrated that the hybrid method is able to dynamically determine what is the most appropriate network reconfiguration and OLTC tap positions to be used each hour, adapting to variable load requirements and renewable generation. But in a real-world distribution end, tie-switch operation and continuous OLTC adjustments are not easily practical because of mechanical wear and tear, reliability issues and coordination of control. In order to cope with this challenge, the suggested methodology proposes the use of a daily configuration strategy such that only one best combination of tie-switches and OLTC tap position is used throughout the 24 h period. Daily set-up (10, 14, 17, 58, 59) and 0.99375 p.u. of the IEEE 69-bus system and (25, 29, 31, 53, 56) and 0.99375 p.u. of the Iran 59-bus system give constant and effective operation at all hours of the day. This approach is unlike

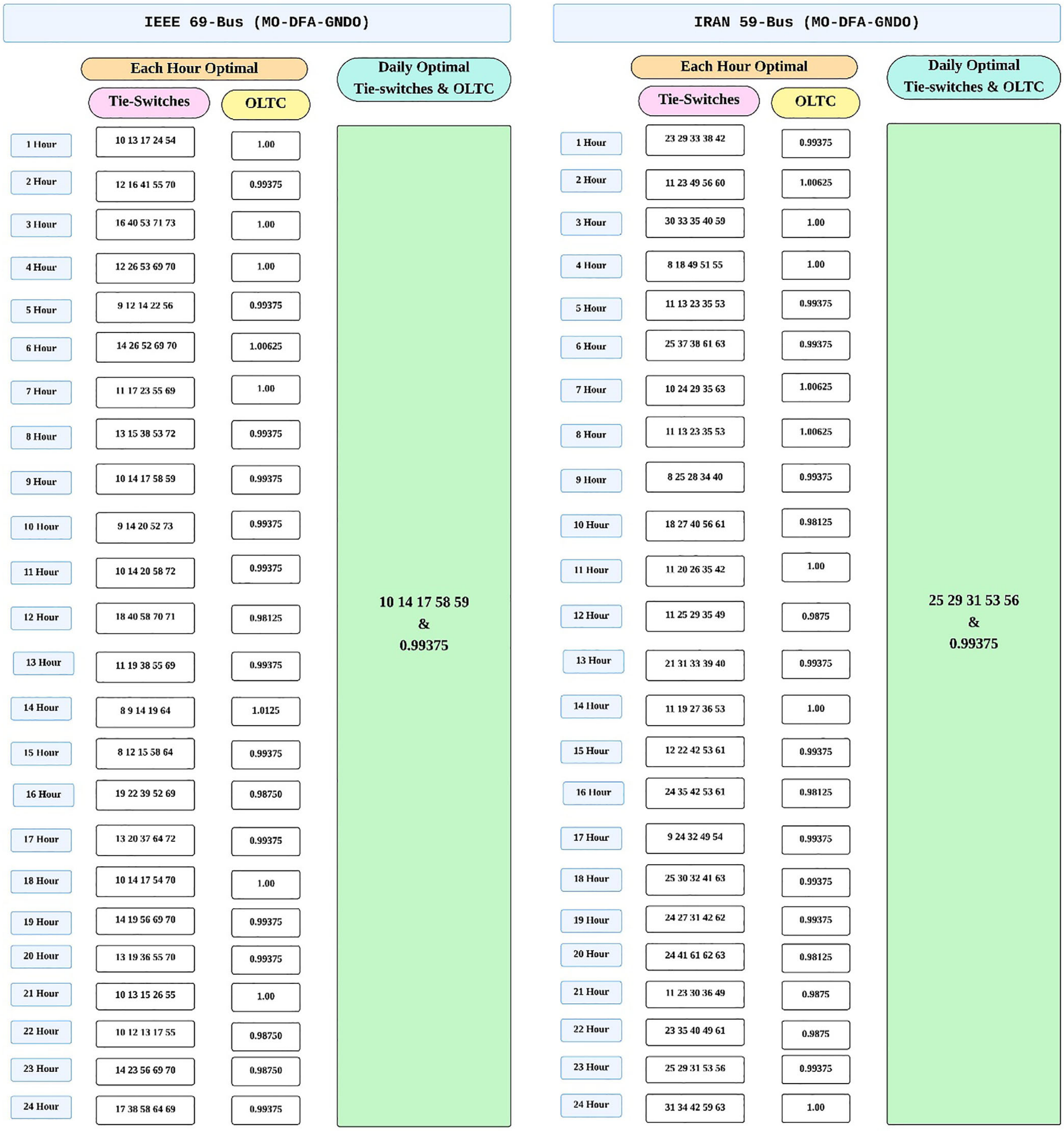

FIGURE 12 | Optimal hourly and daily selection of tie-switches and OLTC settings for IEEE 69-bus and Iran 59-bus systems using Mo-DFA-GNDO.

the traditional process that is called to adjust tie-switches and OLTC settings every hour; it provides a practical implementation and a performance that is close to optimal. The hybrid algorithm is useful in balancing the network loss reduction, improving the voltage profile and saving on operations, and performing system efficiency at a comparative cost of 2–3% of the fully hourly-optimized solution and decreases switching activities by over 95%. In this way, Figure 12 indicates the potential of the offered approach to present a technically sound and operationally viable solution to the distribution networks in the real world.

Figure 13 shows the convergence properties of both algorithms on the basis of hypervolume instrument (HVI) and IGD indices of the IEEE 69-bus test system. These two approaches demonstrate a gradual increase in the quality of a solution as the iterations are executed, although the hybrid approach proposed has more rapid and consistent convergence. The HV curve shows that MO-DFA-GNDO quickly plateaus at about 0.83 in the initial 500 iterations, whereas MOPSO takes almost 3000 steps to achieve a smaller final HV of some 0.79. In the same way, the IGD curve demonstrates that the hybrid approach reaches a lower value of IGD

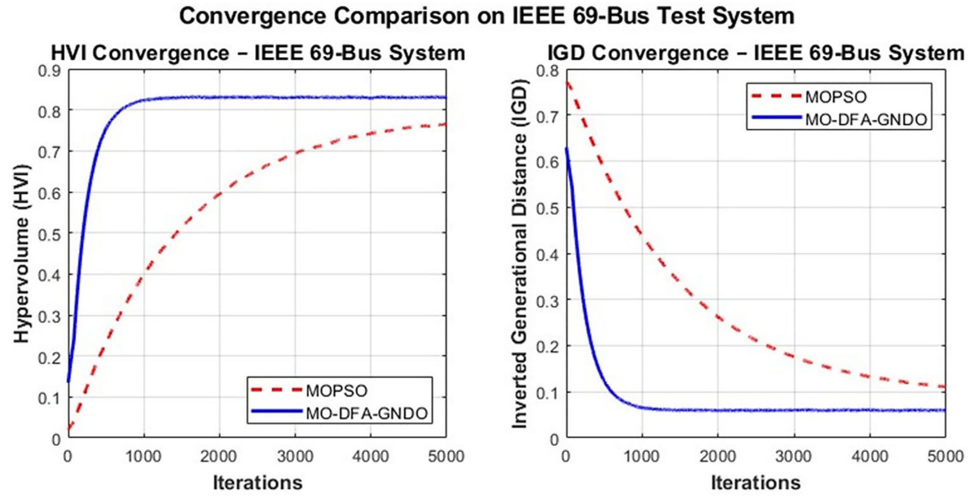

FIGURE 13 | Convergence comparison of MOPSO and hybrid MO-DFA-GNDO for IEEE 69-bus.

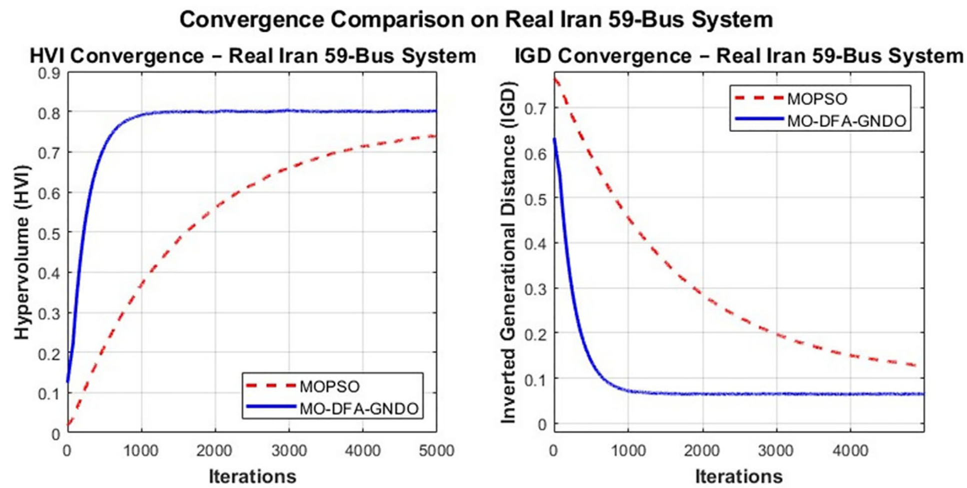

FIGURE 14 | Convergence comparison of MOPSO and hybrid MO-DFA-GNDO for Iran 59-bus.

of approximately 0.06 much sooner, whereas MOPSO reaches its end result of 0.09 progressively. These findings confirm the fact that the hybrid algorithm that is proposed is more efficient in convergence and also better in Pareto-front quality, relative to the traditional MOPSO.

The HVI and IGD convergence curves of the real 59-bus distribution network are presented in Figure 14. The hybrid method of MO-DFA-GNDO proposed is better in rate of convergence and the overall performance as compared to MOPSO. The HVI curve indicates that the hybrid technique reaches a stable state of 0.80 in 600 iterations compared to MOPSO, which takes a longer time of about 3200 to reach its 0.77 value. The hybrid approach will get a final value of approximately 0.065 in terms of IGD performance, and MOPSO will stabilize at approximately 0.10. The similar results of the two test networks support the effectiveness and solidity of the suggested hybrid solution.

Table 3 gives a summary of the convergence of the MOPSO as well as the proposed Hybrid MO-DFA-GNDO algorithm to both test systems as measured by the HVI and IGD measures. The findings are categorical that a hybrid approach converges much faster without compromising Pareto fronts of high quality. Convergence is achieved in 500 iterations in the hybrid method of the IEEE 69-bus system as compared to 3000 iterations in MOPSO, and this implies that the hybrid method is 83.3 times faster than MOPSO in reaching convergence. The obtained results of MOPSO and the suggested MO-DFA-GNDO method demonstrate that the index of the HVI has increased by 0.79 to 0.83, and the index of the IGD has reduced by 0.09 to 0.06, respectively. These advances signify increased variety of solutions and have a closer proximity to the actual Pareto front. On the whole, the findings can confirm that the hybrid approach offers significantly stronger exploration and quicker convergence than the standard MOPSO approach.

5 | Conclusion

In this paper, a hybrid optimization framework is proposed, which is based on the DFA and the GNDO algorithm to organize

TABLE 3 | Convergence performance comparison (HV and IGD metrics).

System	Metric	MOPSO	MO-DFA-GNDO	Improvement
IEEE 69-bus	Iterations to converge	3000	500	83.3% faster
IEEE 69-bus	Final HV	0.79	0.83	+5.1%
IEEE 69-bus	Final IGD	0.090	0.060	−33.3%
Iran 59-bus	Iterations to converge	2800	550	80.4% faster
Iran 59-bus	Final HV	0.77	0.81	+5.2%
Iran 59-bus	Final IGD	0.088	0.062	−29.5%

the planning process and activity of ADNs with intensive coverage of RES. The suggested solution is a collaborative operation in the optimization of RES and BESS and in fulfilling all the realistic operation requirements. The simulations are done on the IEEE 69-bus system and the real Iran 59-bus distribution network. These findings indicate that the suggested approach can yield a reduction in active power loss, voltage deviation and operation cost by up to 87, 96 and 90 percent, respectively, in comparison with the base case. Moreover, the suggested hybrid approach is faster and has a better quality of solution than the MOPSO algorithm. The structure also determines one optimum OLTC, and network reconfiguration setting that minimizes switching operations and maintenance activities by more than 90% over the conventional hourly reconfiguration schemes, which do not work in the real world. These results indicate the strength, effectiveness, and feasibility of the suggested hybrid optimization model in smart active distribution systems. The current study could be further improved in the future by adding demand response programs and multi-timescale coordination approaches to achieve greater flexibility, reliability and resilience of the system.

Author Contributions

Asad Ali: conceptualization, software, writing – review and editing, writing – original draft, methodology, investigation. **Hazlie Mokhlis:** supervision, validation, writing – review and editing, validation, investigation. **Nurulafiqah Nadzirah Mansor:** supervision, validation, writing – review and editing, resources. **Hasmaini Mohamad:** supervision, validation, writing – review and editing, formal analysis. **Nur Zawani Saharuddin:** writing – review and editing, investigation, resources, data curation. **Hussain Shareef:** software, validation, resources, project administration

Acknowledgements

This research was supported by International Research Grant UAE-UM (IF099-2024), Universiti Malaya Research Grant (MG003-2025), and Universiti Teknikal Malaysia Melaka (UTeM) for the funding supported for publication of this paper.

Conflicts of Interest

The authors declare no conflicts of interest.

Data Availability Statement

The data that support the findings of this study are available from the corresponding author upon reasonable request.

References

1. M. Alshehri and J. Yang, "Voltage Optimization in Active Distribution Networks—Utilizing Analytical and Computational Approaches in High Renewable Energy Penetration Environments," *Energies* 17, no. 5 (2024): 1216.

2. G. Justice, G. Nyantakyi, and S. H. Isaac, "The Effect of Renewable Energy on Carbon Emissions Through Globalization," *Heliyon* 10, no. 5 (2024): e26894.

3. M. Farghali, A. I. Osman, Z. Chen, et al., "Social, Environmental, and Economic Consequences of Integrating Renewable Energies in the Electricity Sector: A Review," *Environmental Chemistry Letters* 21, no. 3 (2023): 1381–1418.

4. S. Barakat, H. Ibrahim, and A. A. Elbaset, "Multi-Objective Optimization of Grid-Connected PV-Wind Hybrid System Considering Reliability, Cost, and Environmental Aspects," *Sustainable Cities and Society* 60 (2020): 102178.

5. P. Rani, V. Parkash, and N. K. Sharma, "Technological Aspects, Utilization and Impact on Power System for Distributed Generation: A Comprehensive Survey," *Renewable and Sustainable Energy Reviews* 192 (2024): 114257.

6. T. Song and J. Teh, "Coordinated Integration of Wind Energy in Microgrids: A Dual Strategy Approach Leveraging Dynamic Thermal Line Rating and Electric Vehicle Scheduling," *Sustainable Energy, Grids and Networks* 38 (2024): 101299.

7. M. Mahdavi, H. H. Alhelou, P. Gopi, and N. Hosseinzadeh, "Importance of Radiality Constraints Formulation in Reconfiguration Problems," *IEEE Systems Journal* 17, no. 4 (2023): 6710–6723.

8. M. A. Iqbal and R. Zafar, "A Novel Radiality Maintenance Algorithm for the Metaheuristic Based Co-Optimization of Network Reconfiguration With Battery Storage," *IEEE Access* 11 (2023): 25689–25701.

9. A. Ali, Z. Liu, A. Ali, G. Abbas, E. Touti, and W. Nureldeen, "Dynamic Multi-Objective Optimization of Grid-Connected Distributed Resources along With Battery Energy Storage Management via Improved Bidirectional Coevolutionary Algorithm," *IEEE Access* 12 (2024): 58972–58992.

10. D. Sreenivasulu Reddy and V. Janamala, "Optimal Allocation of Renewable Sources With Battery and Capacitors in Radial Feeders for Reliable Power Supply Using Pathfinder Algorithm," *Journal of Solar Energy Research* 8, no. 4 (2023): 1651–1662.

11. R. Borjali Navesi, D. Nazarpour, R. Ghanizadeh, and P. Alemi, "Switchable Capacitor Bank Coordination and Dynamic Network Reconfiguration for Improving Operation of Distribution Network Integrated With Renewable Energy Resources," *Journal of Modern Power Systems and Clean Energy* 10, no. 3 (2021): 637–646.

12. A. T. Hachemi, F. Sadaoui, A. Saim, M. Ebeed, and S. Arif, "Dynamic Operation of Distribution Grids With the Integration of Photovoltaic Systems and Distribution Static Compensators Considering Network Reconfiguration," *Energy Reports* 12 (2024): 1623–1637.

13. H. M. A. Ahmed, M. H. Ahmed, and M. M. A. Salama, "A Linearized Multiobjective Energy Management Framework for Reconfigurable

Smart Distribution Systems Considering BESSs," *IEEE Systems Journal* 16, no. 1 (2021): 1258–1269.

14. A. Inaolaji, X. Wu, R. Roychowdhury, and R. Smith, "Optimal Allocation of Battery Energy Storage Systems for Peak Shaving and Reliability Enhancement in Distribution Systems," *Journal of Energy Storage* 95 (2024): 112305.

15. L. Hua, X. Junjie, G. Xiang, et al., "Scenario-Based Stochastic Optimization on the Variability of Solar and Wind for Component Sizing of Integrated Energy Systems," *Renewable Energy* 237 (2024): 121543.

16. H. Li, Z. Ren, M. Fan, et al., "A Review of Scenario Analysis Methods in Planning and Operation of Modern Power Systems: Methodologies, Applications, and Challenges," *Electric Power Systems Research* 205 (2022): 107722.

17. Y. Liu, J. Li, and L. Wu, "Coordinated Optimal Network Reconfiguration and Voltage Regulator/DER Control for Unbalanced Distribution Systems," *IEEE Transactions on Smart Grid* 10, no. 3 (2018): 2912–2922.

18. R. Zafar and H. R. Pota, "Multi-Timescale Coordinated Control With Optimal Network Reconfiguration Using Battery Storage System in Smart Distribution Grids," *IEEE Transactions on Sustainable Energy* 14, no. 4 (2023): 2338–2350.

19. L. Wang, X. Wang, C. Jiang, S. Yin, and M. Yang, "Dynamic Coordinated Active–Reactive Power Optimization for Active Distribution Network With Energy Storage Systems," *Applied Sciences* 9, no. 6 (2019): 1129.

20. G. Abbas, Z. Wu, and A. Ali, "Optimal Scheduling and Management of Grid-Connected Distributed Resources Using Improved Decomposition-Based Many-Objective Evolutionary Algorithm," *IET Generation, Transmission & Distribution* 18, no. 16 (2024): 2625–2649.

21. A. Ali, Z. Liu, A. Ali, G. Abbas, E. Touti, and W. Nureldeen, "Dynamic Multi-Objective Optimization of Grid-Connected Distributed Resources Along With Battery Energy Storage Management via Improved Bidirectional Coevolutionary Algorithm," *IEEE Access* 12 (2024): 58972–58992.

22. G. Abbas, Z. Wu, and A. Ali, "Multi-Objective Multi-Period Optimal Site and Size of Distributed Generation Along With Network Reconfiguration," *IET Renewable Power Generation* 18, no. 16 (2024): 3704–3730.

23. J. Liu, Y. Li, C. Rehtanz, et al., "An OLTC-Inverter Coordinated Voltage Regulation Method for Distribution Network With High Penetration of PV Generations," *International Journal of Electrical Power & Energy Systems* 113 (2019): 991–1001.

24. A. A. L. Ahmad, R. Sirjani, and S. Daneshvar, "New Hybrid Probabilistic Optimisation Algorithm for Optimal Allocation of Energy Storage Systems Considering Correlated Wind Farms," *Journal of Energy Storage* 29 (2020): 101335.

25. V. Thapar, G. Agnihotri, and V. K. Sethi, "Critical Analysis of Methods for Mathematical Modelling of Wind Turbines," *Renewable Energy* 36, no. 11 (2011): 3166–3177.

26. J. Zhang, G. Xiong, K. Meng, P. Yu, G. Yao, and Z. Dong, "An Improved Probabilistic Load Flow Simulation Method Considering Correlated Stochastic Variables," *International Journal of Electrical Power & Energy Systems* 111 (2019): 260–268.

27. B. R. Prusty and D. Jena, "A Critical Review on Probabilistic Load Flow Studies in Uncertainty Constrained Power Systems With Photovoltaic Generation and a New Approach," *Renewable and Sustainable Energy Reviews* 69 (2017): 1286–1302.

28. P. Emrani-Rahaghi and H. Hashemi-Dezaki, "Optimal Scenario-Based Operation and Scheduling of Residential Energy Hubs Including Plug-In Hybrid Electric Vehicle and Heat Storage System Considering the Uncertainties of Electricity Price and Renewable Distributed Generations," *Journal of Energy Storage* 33 (2021): 102038.

29. Y.-C. Hung, "A Review of Monte Carlo and Quasi-Monte Carlo Sampling Techniques," *WIREs Computational Statistics* 16, no. 1 (2024): e1637.

30. B. Y. Qu, Y. S. Zhu, Y. C. Jiao, M. Y. Wu, P. N. Suganthan, and J. J. Liang, "A Survey on Multi-Objective Evolutionary Algorithms for the Solution of the Environmental/Economic Dispatch Problems," *Swarm and Evolutionary Computation* 38 (2018): 1–11.

31. N. Khodadadi, E. Khodadadi, B. Abdollahzadeh, et al., "Multi-Objective Generalized Normal Distribution Optimization: A Novel Algorithm for Multi-Objective Problems," *Cluster Computing* 27, no. 8 (2024): 10589–10631.

32. R. Azimi and S. Esmaeili, "Multiobjective Daily Volt/VAR Control in Distribution Systems With Distributed Generation Using Binary Ant Colony Optimization," *Turkish Journal of Electrical Engineering and Computer Sciences* 21, no. 3 (2013): 613–629.

33. A. Lotfipour and H. Afrakhte, "A Discrete Teaching–Learning-Based Optimization Algorithm to Solve Distribution System Reconfiguration in Presence of Distributed Generation," *International Journal of Electrical Power & Energy Systems* 82 (2016): 264–273.